

# Organic/Inorganic bioactive materials Part II: *in vitro* bioactivity of Collagen-Calcium Phosphate Silicate/Wollastonite hybrids

Research Article

Lachezar Radev\*, Vladimir Hristov, Bisserka Samuneva, Dimitrina Ivanova

University of Chemical Technology and Metallurgy,  
1756 Sofia, Bulgaria

Received 4 December 2008; Accepted 13 March 2009

**Abstract:** In the present study, novel hybrid materials of Collagen (C) and Calcium Phosphate Silicate/Wollastonite (CPS/W) were synthesized. The CPS/W ceramic was prepared *via* polystep sol-gel method. The dissolution test of CPS/W ceramic was filled with TRIS-HCl buffer. FTIR depicts that hydroxyl carbonate apatite ( $\text{OHCO}_3\text{HA}$ ) was observed after 3 days of immersion in TRIS-HCl buffer. Biohybrids of C-CPS/W were produced from diluted hydrochloric acid collagen type I and ceramic powder with different ratios of C and CPS/W equal to 25:75 and 75:25 wt.%. The synthesized hybrids were characterized by FTIR, XRD and SEM. FTIR depicts a “red shift” if amide I could be attributed to the fact that the collagen prefers to chelate  $\text{Ca}^{2+}$  from partial dissolution of CPS/W ceramic. The growth of B-type carbonate containing hydroxyapatite (B- $\text{CO}_3\text{HA}$ ) on the C-CPS/W hybrids soaked in 1.5SBF was observed. The negatively charged carboxylate groups from the collagen may be responsible for hydroxyapatite (HA) deposition. This fact was confirmed by the “red shift” of carboxylate groups of collagen in FTIR spectra. The formation of HA was observed by FTIR, XRD and SEM.

**Keywords:** Collagen • Calcium phosphate silicate/wollastonite • Biohybrids

© Versita Warsaw and Springer-Verlag Berlin Heidelberg.

## 1. Introduction

Bone tissue engineering is a new research area with a wide variety of clinical applications in bone replacement on orthopedic defects, bone neoplasia, pseudoarthrosis treatment, stabilization of spinal segments, as well as in maxillofacial, craniofacial, orthopedic, reconstructive, trauma and neck and head surgery [1].

During the last decades, different biomaterials of biological or synthetic origin have been designed, aiming to act as extracellular matrix scaffolds for new bone formation. Clinical uses require a series of biomedical properties, such as bioactivity, osteoconduction, osteoinduction, biocompatibility and biodegradation; besides they should be cheap, easily produced, molded and stored [2,3].

Hydroxyapatite (HA) is one of the frequently used bioceramics for bone and dental tissue reconstitution. It has excellent biocompatibility with hard tissues [4], and high osteoconductivity and bioactivity despite its low degradation rate [5], mechanical strength and osteoinductive potential [5,6]. In these fields of knowledge, glass-ceramics in ternary ( $\text{CaO-SiO}_2\text{-P}_2\text{O}_5$ ) systems have also been examined for biomedical [7-13] and ceramic hybrid applications [14] due to their good chemical and mechanical properties. Collagen is biocompatible, biodegradable and osteoinductive, acting as an excellent delivery system for bone morphogenetic proteins [15,16]. When associated to ceramic particles forming a biocomposite, it prevents the ceramic dispersion in implants, resulting in an easily molded biomaterial [17]. Bovine collagen antigenicity may be reduced by treatments with pepsin and strong alkaline

\* E-mail: l\_radev@abv.bg

solutions, and physicochemical agents that induce cross-linking of collagen [16]. The HA embedded collagen nanostructure has been reproduced by a self-organization reaction of HA nanocrystals using a biomimetic co-precipitation method by using  $\text{Ca}(\text{OH})_2$ ,  $\text{H}_3\text{PO}_4$  and collagen [18-25]. In order to give the strength, HA/collagen nanocomposite were cross-linked by using glutaraldehyde (GA) [19,20,26,27] and chondroitinsulfate (ChS) [21,28]. As a result, the cross-linking induced a significant structure development from nanoscale range to microscale range. The GA and ChS play important roles in controlling the function of osteoblast [29,30]. Some authors described on the possibility to obtain collagen/HA and collagen/wollastonite scaffolds *via* a freeze-drying technique. This method involves freezing an aqueous dispersion of collagen HA or wollastonite, which leads to the aggregation of these components in the interstitial spaces of the ice crystal network, generating a porous structure. The ice is then removed by sublimation, leaving a foamed collagen matrix embedded with HA or wollastonite particles [31,32]. Nano-patterned collagen layers on a sintered and polished HA disk were prepared by Monkawa *et al.* [33] by using a dewetting process. The nano-patterned collagen layer on HA disk was obtained by a slow-drying process at 95% humidity for 2 days. The composite fibers between collagen and HA were produced by electrospinning to fabricate hybrid nanofibres [34] with the perfect orientation of HA along the collagen matrix.

In recent years, there has been some information in the literature about the synthesis and bioactive properties of monophasic HA mixed with collagen to produce bioactive composites with interesting properties [35-37]. Other authors studied the possibility to produce bioactive materials between biphasic Hydroxyapatite/Tricalcium Phosphate (HA/TCP) ceramics and type I collagen for filling intramedullary cavities remaining after tumor excision [38], dehiscence-type defects in dogs [39], bone tissue regeneration [40] and rebuilding small lesions in bone tissue engineering [41].

To date, there is no information in the literature about synthesis and *in-vitro* bioactivity of collagen (C) and calcium phosphate silicate/wollastonite (CPS/W) hybrids.

The aim of this work was to synthesize organic-inorganic hybrids and to evaluate their *in-vitro* bioactivity in 1.5 SBF. First, we synthesized CPS/W ceramics as described in [42]. Second, we studied the dissolution behavior of new CPS/W bioactive ceramics in TRIS-HCl buffer. Third, we synthesized two series of collagen C-CPS/W hybrids with various amounts of them. We describe the obtained hybrids as C-CPS/W-

25:75 wt.% and C-CPS/W-75:25 wt.%, where 25 and 75 are wt.% of C and new CPS/W glass-ceramic was used for the preparation of the hybrids. A series of C-CPS/W hybrids was prepared by a mixing procedure without the use of cross-linkage. Fourth, we evaluate *in vitro* bioactivity of the prepared CPS/W glass-ceramics and C-CPS/W hybrids using 1.5 SBF.

## 2. Experimental Part

### 2.1. Preparation of the glass-ceramic sample

The inorganic material, part of the prepared hybrids, has been synthesized by polystep sol-gel method.

The procedure for the synthesis and structure evolution of the obtained samples is documented in [42].

### 2.2. Dissolution test of glass-ceramic sample in TRIS-HCl buffer

The dissolution test of obtained glass-ceramic was carried out in TRIS-HCl buffer. Briefly, the amount of TRIS-(hydroxymethyl) aminomethane  $(\text{CH}_2\text{OH})_3\text{CNH}_2$  powder necessary to obtain a solution 1M was dissolved in water, and the pH was adjusted to a value of  $\sim 7.4$  with HCl 2M. The desired amount of CPS/W powders (0.5 g) was dissolved in a beaker with 50 cm<sup>3</sup> of the TRIS-HCl solution as prepared, in a static condition at room temperature. The dissolution experiments went on for 3 days for the samples. After 3 days of reaction in TRIS-HCl, the bulk CPS/W samples were washed in water and dried in an oven at 70°C for 4 h.

### 2.3. Preparation of the organic/inorganic hybrids

The C-CPS/W hybrids for two types of proportions 25:75 and 75:25 wt.% were prepared by adding the inorganic phase powder (CPS/W) to the collagen (Fluka), diluted in 0.1N HCl. Initially collagen type I (Fluka), taken in amounts corresponding to the hybrid content, was diluted in 20 mL 0.1N HCl for 24 h at room temperature. Collagen I concentration in the obtained solutions was 0.0045 g mL<sup>-1</sup> and 0.013 g mL<sup>-1</sup>, calculated on the basis of dry hybrid with weight equal to 0.7 g. After homogenization time, the finely powdered CPS/W glass-ceramic, in amounts corresponding to the hybrid content, was added to the diluted collagen I at continuing intensive stirring. The homogenization time was for 6 h. pH was adjusted at 9 using 25%  $\text{NH}_4\text{OH}$ . 0.5 ml 0.01% sodium azide was added to the mixed xerogel to prevent bacterial growth [43]. The obtained hybrid materials were dried at 37°C/12 h under vacuum.

## 2.4. *In vitro* assessment of bioactivity in 1.5 SBF

Bioactivity of obtained C-CPS/W hybrid materials was evaluated by examining the apatite formation on their surfaces in 1.5 SBF. 1.5 SBF solution was prepared from reagents as follows: NaCl=11.9925 g, NaHCO<sub>3</sub>=0.5295 g, KCl=0.3360 g, K<sub>2</sub>HPO<sub>4</sub>·3H<sub>2</sub>O=0.3420 g, MgCl<sub>2</sub>·6H<sub>2</sub>O=0.4575 g, CaCl<sub>2</sub>·2H<sub>2</sub>O=0.5520 g, Na<sub>2</sub>SO<sub>4</sub>=0.1065 g, and buffering at pH 7.4 at 36.5°C with TRIS=9.0075 g and 1M HCl in distilled water. C-PCS/W hybrids were pressed at 50 MPa with PVA to disc (12×2 mm) specimens and immersed in 1.5 SBF at human body temperature (36.6°C) in polyethylene bottles in static conditions for 3 days. After soaking, the specimens were removed from the fluid and gently rinsed with distilled water, and then dried at 37°C/6 h [44].

## 2.5 Measurements and observations

The structure and *in vitro* bioactivity of CPS/W glass-ceramics and C-CPS/W hybrids were monitored by XRD, FTIR and SEM.

Powder X-ray diffraction spectra were collected within the range from 10° to 8° 2θ with a constant step 0.04° 2θ and counting time 1s/step on Bruker D8 Advance diffractometer with CuK<sub>α</sub> radiation and SolX detector. The spectra were evaluated with the *Diffraplus* EVA package.

On the dry ceramic powders and organic/inorganic hybrids, FTIR transmission spectra were recorded using a Bruker Tensor 27 spectrometer with scanner velocity 10KHz. KBr diluted pellets were prepared by mixing ~1 mg of the samples with 300 mg KBr. Transmission spectra were recorded using MCT detector, with 64 scans and 1 cm<sup>-1</sup> resolution.

Morphological studies of the obtained glass-ceramics and hybrids before and after immersion in 1.5 SBF was

done by using SEM. The samples were gold-sputter coated and viewed in the secondary electron mode with a field emission gun Scanning electron microscope (Phillips-515) operated at an accelerating voltage of 2.5 kV.

## 3. Results and Discussion

### 3.1. X-ray diffraction (XRD)

XRD patterns of the prepared dried and thermal treated at 1200°C/2 h are given in Fig. 1.

XRD proved the presence of Ca<sub>15</sub>(PO<sub>4</sub>)<sub>2</sub>(SiO<sub>4</sub>)<sub>6</sub> (PDF 50-0905), β-CaSiO<sub>3</sub> (pseudowollastonite) (PDF 74-0874) and α-CaSiO<sub>3</sub> (wollastonite) (PDF 84-0655). The obtained XRD data for the prepared Ca<sub>15</sub>(PO<sub>4</sub>)<sub>2</sub>(SiO<sub>4</sub>)<sub>6</sub> is in very good agreement with Mumme *et al.* [45]. As can it is known, CaO and P<sub>2</sub>O<sub>5</sub> might move to SiO<sub>2</sub> to form a Ca-Si-P-O glassy phase [46]. For HA/W = 25/75 wt.% sample, after annealing at 1350°C/2 h, Ryu *et al.* [47] observed the presence of Ca<sub>12</sub>P<sub>2</sub>Si<sub>6</sub>O<sub>31</sub> phase. Barba *et al.* established the presence of Ca<sub>7</sub>P<sub>2</sub>SiO<sub>16</sub> in the calcium phosphate ceramics after thermal treatment at 1150°C/2 h [48].

### 3.2. Dissolution test in TRIS-HCl buffer

It is generally accepted that the mechanism of reactivity of glass-ceramics as implants is quite complex. It involves both “inorganic” reactions, such as dissolution and precipitation of some glass-ceramics components, and “biological” interactions with proteins and cells.

We focused on the analysis of the early stage of reactivity of CPS/W glass-ceramics, as it is logical to assume that the earliest stage of the reaction will have a profound influence on the subsequent stages of the glass surface reactions, and ultimately the bioactivity of the material. We want to analyze the dissolution and

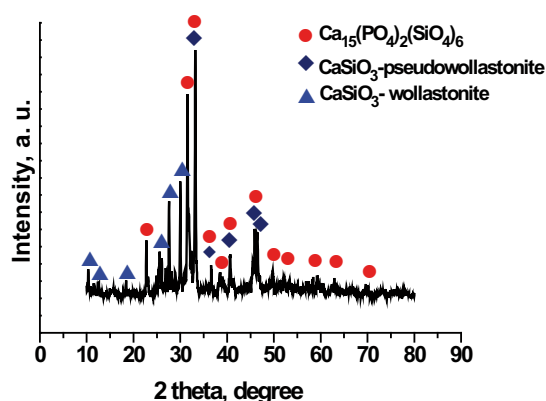


**Figure 1.** XRD patterns for the obtained calcium phosphate silicate, annealed at 1200°C/2 h

re-precipitation process involving CPS/W glass-ceramics alone, and for this reason we did not want to use SBF, because they have a high concentration of calcium, phosphorus and other ions that could easily precipitate in the presence of just a few nucleation sites. It is important to highlight, however, that we studied the reaction of new CPS/W glass-ceramics in a very simple model, *i.e.* distilled water buffered with TRIS and hydrochloric acid. The obtained CPS/W glass-ceramics were immersed in TRIS-HCl buffer for 3 days.

FTIR spectroscopy was used to study the obtained materials after a heat treatment state and to quantify the effect of silicon substitution in prepared calcium phosphate silicate ceramic and to evaluate the changes with the sample after being immersed in TRIS-HCl buffer for 3 days.

FTIR spectra of thermal treated CPS/W and CPS/W after immersion in TRIS-HCl buffer are given in Figs. 2a,b.

As can be seen, the obtained FTIR spectrum of the thermal treated sample, before soaking in TRIS-HCl buffer (Fig. 2a), is very complicated. From the literature data, the intense bands at 568, 600, 960, 1043 and 1008  $\text{cm}^{-1}$  correspond to  $\nu_4$ ,  $\nu_1$  and  $\nu_3$  P-O stretching vibration modes [49]. The FTIR spectrum of the thermal treated sample had characteristic  $\nu_3$   $\text{PO}_4^{3-}$  and  $\nu_1$   $\text{PO}_4^{3-}$  bands, identified by the three peaks at 1020, 1067 and 987  $\text{cm}^{-1}$  [50-53]. On the other hand the absorption bands and 1020 and 1067  $\text{cm}^{-1}$  can be assigned to the vibration of the  $\nu_{\text{as}}$  Si-O-Si bond [54]. The  $\nu_4$   $\text{PO}_4^{3-}$  was identified by some peaks, centered at 520, 651  $\text{cm}^{-1}$  [50-53]. In the sample, we can observe the presence of one peak, centered at  $\sim 460$   $\text{cm}^{-1}$  which could be

ascribed to  $\nu_2$   $\text{PO}_4^{3-}$  [50,53]. As can be seen, only one peak, centered at 943  $\text{cm}^{-1}$  was detected. This peak can be assigned to the presence of  $\text{SiO}_4^{4-}$  in the prepared sample [55]. The peaks centered at 405, 428, 453, 562 and 718  $\text{cm}^{-1}$  could be ascribed to the presence of wollastonite and pseudowollastonite [56-59]. In this context, Dong *et al.* described that the peaks, centered at 405 and 453  $\text{cm}^{-1}$  are associated with the presence of  $\nu$ Si-O-Ca in the wollastonite structure [59]. As can be seen, the OH stretch at 3415  $\text{cm}^{-1}$  dramatically decreases with the addition of silicon in the obtained sample. A very surprising result in this sample is the presence of slight  $\text{CO}_3^{2-}$  band, which is observed at 1419 and 1489  $\text{cm}^{-1}$  [50-52,60,61]. A  $\text{CO}_3^{2-}$  presence in the samples is due to absorbance of  $\text{CO}_2$  from the air even after thermal treatment at 1200°C/2 h, *i.e.* CPS/W sample must be kept out of the atmosphere in a desiccator [42].

To have a confirmation of the changes going on with the synthesized CPS/W sample, we scanned the FTIR spectrum after its immersion in TRIS-HCl buffer for 3 days. This FTIR spectrum is shown in Fig. 2b. As can be seen, the bands, centered at 401, 461 and 473  $\text{cm}^{-1}$ , which are assigned to the presence of  $\nu$ Si-O-Ca in the wollastonite structure [59] have a very small intensity after immersion for 3 days. In the presented spectrum, a new peak appears at 800  $\text{cm}^{-1}$ . This peak is assigned to the presence of  $\text{SiO}_2$  ( $\delta$  Si-O-Si) [62]. On the other hand, the FTIR spectrum shows that the 901  $\text{cm}^{-1}$  flexible vibration of  $\nu$ Si-O becomes weak and the 1068  $\text{cm}^{-1}$  peak is gradually clear. The peak, centered at 1018  $\text{cm}^{-1}$  ( $\nu$ O-Si-O) slightly decreased. The analysis indicates that O-Si-O and Si-O-Ca groups are exposed and gradually transferred into the surface groups of

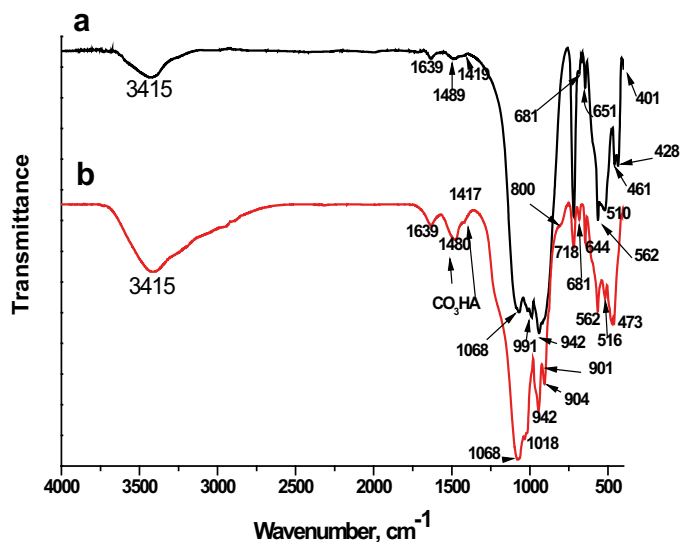


**Figure 2.** FTIR spectra of CPS/W thermal treated at 1200°C/2 h (a) and after immersion in TRIS-HCl buffer for 3 days (b)

SiO<sub>2</sub> in the TRIS-HCl etching process. These results are in a good correspondence with those published by Dong *et al.* [59]. In our case, the band relative to the presence of calcium phosphate is located at 644 cm<sup>-1</sup> [50-53]. The relative intensity of this peak, with respect to the bands, centered at 461 and 800 cm<sup>-1</sup>, are sharper and slightly visible. This could suggest that the relative thickness of the Ca/P rich layer, which is formed after the reaction between glass-ceramic and TRIS-HCl, is greater on larger sized particles in CPS/W ceramic. Interestingly, a similar result was obtained by Cerruti *et al.* [63] in the case of dissolution of Bioglass® in TRIS-HCl buffer for 3 days. An interesting observation in the scanned FTIR spectrum, is that the intensity of the band centered at 718 cm<sup>-1</sup> [56-58] slightly decreased after immersion of the sample in TRIS-HCl buffer, *i.e.* the wollastonite remarkably dissolved in TRIS-HCl buffer for the immersion time.

Moreover, in the obtained FTIR spectrum, we can observe that the intensity of the band centered at 942 cm<sup>-1</sup>, assigned from some authors, to Si-O-Ca vibration mode [64], slightly increases after soaking the CPS/W ceramics in TRIS-HCl buffer. The increasing intensity of this absorption band could be assigned to the presence of chemisorbed Ca<sup>2+</sup> (realized to the media from CPS/W ceramic) during the soaking time (3 days) with rehydrated silica surface (Si-OH groups) of the sample. On the basis of the obtained data, we suppose that the grafting reaction between the Ca species and the silica surface can be observed *via* non-bridging oxygen, *i.e.*  $2\text{Si-OH} + \text{Ca}^{2+} \rightarrow \text{Si-O-Ca}^{2+}\text{-O-Si} + 2\text{H}^+$ . This phenomenon was studied by M. Cerruti *et al.* [65] in the case of sol-gel derived 58S and 77S bioglasses, immersed in SBF for different periods of time. Furthermore, we suppose that the PO<sub>4</sub><sup>3-</sup> (dissolved from ceramics in TRIS-HCl buffer after soaking) are migrated to the Si-O-Ca<sup>2+</sup>-O-Si fragments and formed a calcium phosphate rich layer on the ceramic surface.

On one hand, some authors described that the presence of a distinct and sharp absorption band, centered at 562 cm<sup>-1</sup>, can be assigned to the presence of crystalline calcium phosphates on the ceramic surface [66]. On the other hand, additional characteristic bands from the hydroxylcarbonateapatite (OHCO<sub>3</sub>HA) layer are three bands, centered at about 1417, 1480 and 1636 cm<sup>-1</sup>, assigned to C-O stretching vibration and one about 904 cm<sup>-1</sup>, which could be assigned to C-O out-of-plane bending vibrations of CO<sub>3</sub><sup>2-</sup> groups [7,53]. The presence of carbonate is attributed to the carbonation process of the immersed ceramics due to the atmospheric CO<sub>2</sub> as a consequence of the high calcium content in the TRIS-HCl solution [67].

### 3.3. Formation of C-CPS/W hybrids

To study the processes of eventual interactions between collagen and calcium phosphate silicate/wollastonite ceramics, the FTIR spectra of pure collagen and C-CPS/W (Fig. 3) were compared.

In the spectrum of pure collagen (Fig. 3a), the amide I peak, centered at 1656 cm<sup>-1</sup> predominantly corresponds to the C=O stretch vibration [31,41]. In additional studies [26,41] the amide I band in a bone spectrum is representative of the collagen content and structure. The amide II, positioned at 1550 cm<sup>-1</sup>, corresponds to a combination of the N-H in-plane bend and the C-H stretch vibrations [26]. For the amide III bands there are two bands assigned at 1241 and 1281 cm<sup>-1</sup>. The amide III peaks corresponds to a combination of the C-N stretch and the N-H in-plane bends [31,41]. Amide B is centered at 3081 cm<sup>-1</sup> [31,41,68]. Two additional bands, visible at 1399 and 1340 cm<sup>-1</sup>, can be attributed to the presence of COOH and COO<sup>-</sup> in the spectrum of pure collagen and pure gelatin [69]. Furthermore, there are two distinct changes when the spectrum of pure collagen (Fig. 3a) and C-CPS/W (Figs. 3b,c) were compared. First, the intensity of amide II decreased, while amide III almost disappeared. Second, the amide I peak, observed for pure collagen and centered at 1656 cm<sup>-1</sup>, shifted to 1638 cm<sup>-1</sup> (Fig. 3b) and 1647 cm<sup>-1</sup> (Fig. 3c). From the obtained FTIR results we can assume that the collagen prefers to chelate Ca<sup>2+</sup> from the partially dissolved CPS/W ceramics in the preparing conditions (the characteristic bands belong to SiO<sub>2</sub>, centered at 800 cm<sup>-1</sup> and νSi-O, centered at 963 cm<sup>-1</sup>, can also be observed [59]). The "red shift" of amide I peak indicates that the C=O bonds in the peptide chain were weakened because the formation of new chelate bonds between Ca<sup>2+</sup> and C=O bond. This indicates that the carbonyl groups on the surface of the collagen are the binding sites of Ca<sup>2+</sup> [70]. As it was reported earlier [44], the carbonyl oxygen has a nonbonding free electron pair and it is therefore possible for carbonyl oxygens to chelate some metal ions with empty electron orbitals. It is reasonable to assume that the chelate bond of Ca<sup>2+</sup> is not stronger than that of other metal ions, such as Zn<sup>2+</sup>, Ni<sup>2+</sup> and Co<sup>2+</sup>, but Ca<sup>2+</sup> may chelate several carbonyl groups to form a stable coordination. From Fig. 3 the special future of the amide B does not show a strong modification based on the preparation route of the C-CPS/W hybrids, *i.e.* the conformation change in the secondary structure of the collagen cannot be observed. Chang *et al.* [26] observed the strong modification of amide B in the presence of different quantities of glutaraldehyde (GA) for hydroxyapatite/collagen composites, prepared *via* simultaneous titration method. In the FTIR spectra of C-CPS/W, presented in Fig. 3 curves b and c, we can

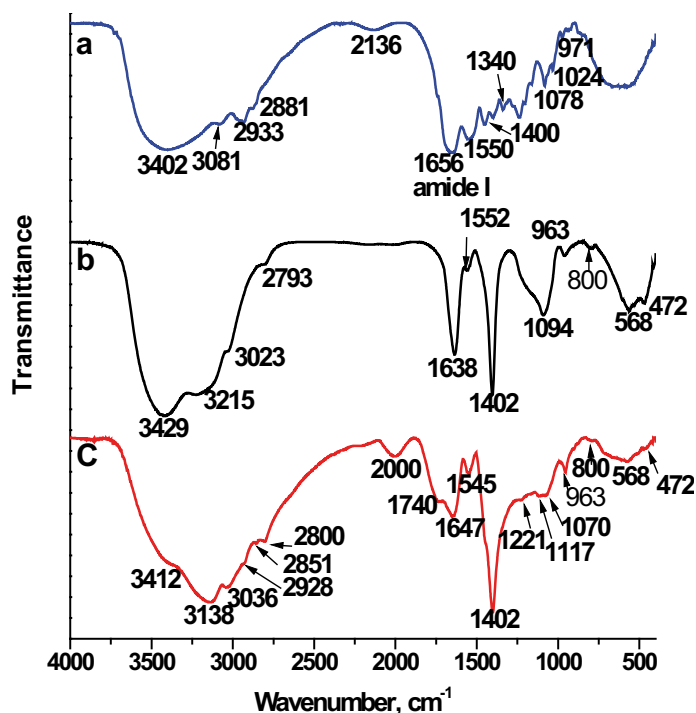


**Figure 3.** FTIR spectra of pure collagen (a), C-CPS/W-25:27 wt.% (b) and C-CPS/W-75:25 wt.% (c)

also depict the presence of  $\nu_2$   $\text{CO}_3^{2-}$  mode, centered at  $\sim 880$   $\text{cm}^{-1}$ , which indicates that the synthesized hybrids were similar to the natural bone [50,51,53,60,71]. On the basis of the obtained results and its interpretation we came to the conclusion that we had prepared biohybrid materials.

Depicted in Fig. 3 (curves b and c), from spectra of the prepared C-CPS/W hybrids we could evaluate the possibility of an interfacial bond between collagen and the inorganic part of the hybrids, *i.e.* CPS/W ceramic. From the O-P-O bending mode ( $\nu_4$   $\text{PO}_4^{3-}$  at  $568$   $\text{cm}^{-1}$ ) and P-O stretching modes ( $\nu_1$   $\text{PO}_4^{3-}$  at  $963$   $\text{cm}^{-1}$ ,  $\nu_2$   $\text{PO}_4^{3-}$  at  $472$   $\text{cm}^{-1}$  and  $\nu_3$   $\text{PO}_4^{3-}$  at  $1070$   $\text{cm}^{-1}$ ) it is considered that the presence of  $\nu_3$   $\text{PO}_4^{3-}$  is the indicator of the amount of inorganic part of the hybrids. As it is known, the presence of  $\nu_1$   $\text{PO}_4^{3-}$  and  $\nu_2$   $\text{PO}_4^{3-}$  reflects on the rate of crystallinity of the prepared glass-ceramics. From the obtained FTIR spectrum it can be also seen that there is a kind of P-O-H bending mode, centered at  $1221$   $\text{cm}^{-1}$ . The presence of this mode reflects the inorganic coordination with the collagen in the prepared hybrid. In the spectrum we can also observe the presence of one mode, centered at  $800$   $\text{cm}^{-1}$ . This mode is specific for the ceramic part of the hybrids, which is annealed at higher temperature and soaked in acid media for the preparation time. In our case, the presence of depicted modes could be assigned on a basis of two processes. First, partial denaturation of the collagen due to using

of  $\text{NH}_4\text{OH}$  for preparation of the hybrids; and second, partial dissolution due to addition of soluble collagen CPS/W ceramic to the acid for 6 h.

### 3.4. In vitro assessment of bioactivity of C-CPS/W hybrids

The FTIR spectra of prepared C-CPS/W hybrids after 3 days immersion in 1.5 SBF are given in Fig. 4

As can be seen, the spectra contained various bands from respective  $\text{PO}_4^{3-}$  groups at  $1069$  and  $1081$   $\text{cm}^{-1}$  (for  $\nu_3$   $\text{PO}_4^{3-}$  and  $\nu_{\text{as}}$  Si-O-Si) [50-52,71],  $452$ ,  $465$  and  $961$   $\text{cm}^{-1}$  (for  $\nu_1$   $\text{PO}_4^{3-}$ ) [50,51,53,67,71-73],  $567$  and  $675$  (for  $\nu_4$   $\text{PO}_4^{3-}$ ) [67,72-75],  $795$  and  $802$   $\text{cm}^{-1}$  (for  $\text{SiO}_4^{4-}$ ,  $\nu_2$   $\text{CO}_3^{2-}$ ) [67,72,73] and OH- groups at  $3418$   $\text{cm}^{-1}$  [52,71].

The  $1340$   $\text{cm}^{-1}$  in collagen (Fig. 3a) that not only represents the carboxyl group, but it is one of a number of bands in the range  $1400$ - $1290$   $\text{cm}^{-1}$ , which are attributed to the presence of type I collagen in biological tissue [76]. The band at  $1340$   $\text{cm}^{-1}$  in collagen is predominantly attributed to the so-call wagging vibration of proline side chains [77]. As shown in Fig. 4b we confirm the “red shift” of this band for the synthesized C-CPS/W materials after immersion in 1.5 SBF. The band, centered at  $1336$   $\text{cm}^{-1}$  can be shown in a wagging vibration through the covalent bond formation with  $\text{Ca}^{2+}$  of partial dissolution of CPS/W ceramic in SBF solution, embedded into the collagen matrix. It is known that the carboxylic groups in collagen are in ionic form in that medium, which is

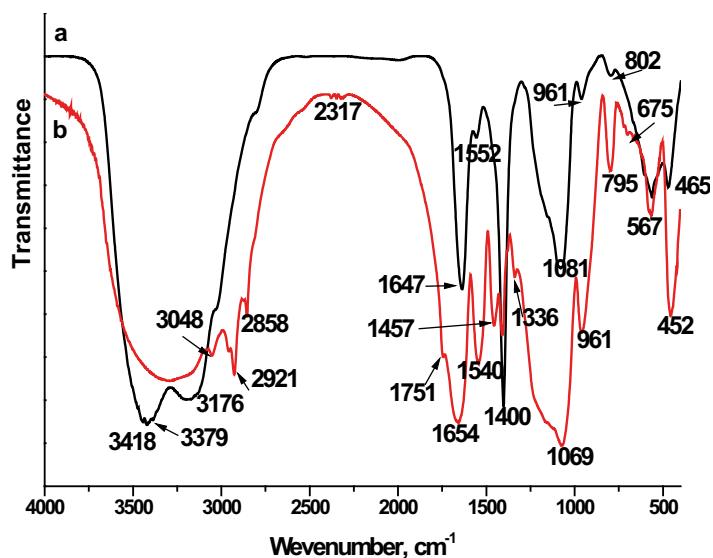


**Figure 4.** FTIR spectra of C-CPS/W hybrids with different quantity of C and CPS/W- 25:75 wt.% (a) and 75:25 wt.% (b), after 3 days immersion in 1.5 SBF

appropriate for binding sites with calcium [26,69]. As can be seen, the asymmetric stretching vibration of the above mentioned carboxylate anions ( $\text{COO}^-$ ), observed in pure collagen at  $1340\text{ cm}^{-1}$  (Fig. 3a), shifted to lower wave number in the case of the hybrid (Fig. 4b). The amount of “red shift” is determined by preparation conditions, such as pH, temperature and concentration of the reagents [69]. In our case, the “red shift” is not influenced by the concentration of two different parts of the hybrid. Our conclusions are in a good correspondence with other literature [26,69,77-79]. As can be seen in the depicted FTIR spectra, the presence of an absorption bands at  $1457\text{ cm}^{-1}$  (Fig. 4b),  $1400\text{ cm}^{-1}$  (Figs. 4a,b) and  $795\text{ cm}^{-1}$  (Fig. 4b) and  $802\text{ cm}^{-1}$  (Fig. 4a) indicated the formation of B-type substituted hydroxyapatite (B-type  $\text{CO}_3\text{HA}$ )

in which  $\text{CO}_3^{2-}$  substituted  $\text{PO}_4^{3-}$  [80]. Furthermore, we can assume that the SBF can re-arrange collagen from the obtained hybrids and partially dissolved CPS/W ceramics, which leads to the super saturation of SBF solution and to the formation of bioapatite on the surface of the hybrids. If  $\text{Ca}^{2+}$  meets with  $\text{PO}_4^{3-}$  it will make HA crystals *via* homogeneous reaction. If  $\text{COO}^-$  reacts with  $\text{Ca}^{2+}$ , the nucleation mechanism of HA formation is heterogeneous. Afterwards,  $\text{PO}_4^{3-}$  will accumulate at the calcium complexes and grow to the critical size of nucleation.

As can be seen, the FTIR spectra of the synthesized and immersed in 1.5 SBF C-CPS/W hybrids exhibit the main collagen and calcium phosphate silicate bands, which are summarized in Table 1.

**Table 1.** Infrared band assignment of  $\text{CO}_3\text{HA}$  on the synthesized C-CPS/W hybrids after immersion in 1.5 SBF

Frequency, $\text{cm}^{-1}$	Assignment	Literature
3048	Amide B	[31,41,68]
2921	C-H stretch	[31,41]
2858	C-H stretch	[31,41]
1654, 1647	C=O stretch (amide I)	[26,31,41]
1540, 1552	N-H in-plane deformation plus C-N stretch (amide II)	[26,31,41]
1457	$\text{CH}_2$ deformation and $\text{CH}_3$ asymmetric deformation	[31,41]
1400	$\nu_2 \text{CO}_3^{2-}$	[67,72,73,80]
1336	$\text{COO}^- \text{Ca}^{2+}$	[26,69,77-79]
1069, 1081	$\nu_3 \text{PO}_4^{3-}$ , $\nu_{\text{as}} \text{Si-O-Si}$	[50-52,71]
961	$\nu_1 \text{PO}_4^{3-}$	[50,51,53,67,71-73]
795, 800	$\text{SiO}_4^{4-}$ , $\nu_2 \text{CO}_3^{2-}$	[67,72,73,80]
670	$\nu_4 \text{PO}_4^{3-}$	[67,72-75]
567	$\nu_4 \text{PO}_4^{3-}$	[67,72-75]
452, 465	$\nu_1 \text{PO}_4^{3-}$	[50,51,53,67,71-73]

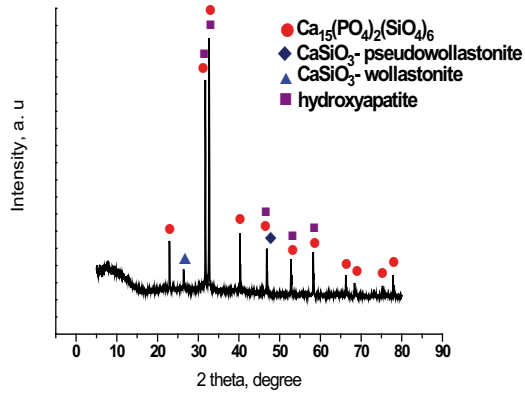


**Figure 5.** XRD of C-CPS/W (25:75 wt.%) after immersion in 1.5 SBF

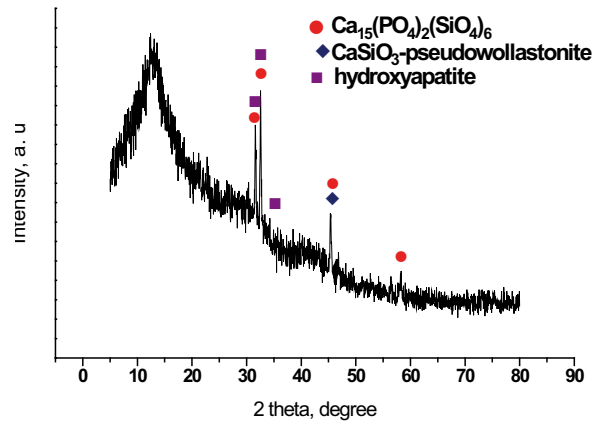


**Figure 6.** XRD of C-CPS/W (75:25 wt.%) after immersion in 1.5 SBF

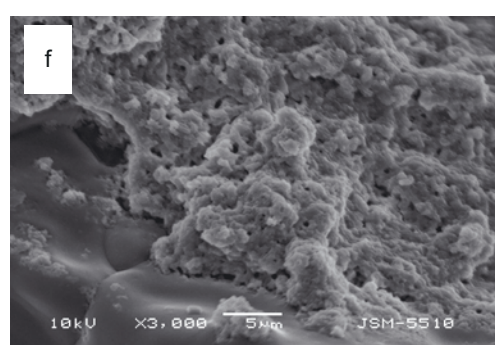
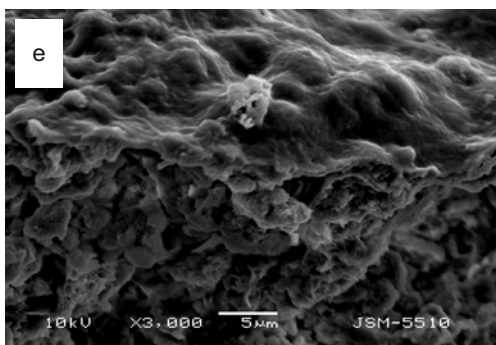
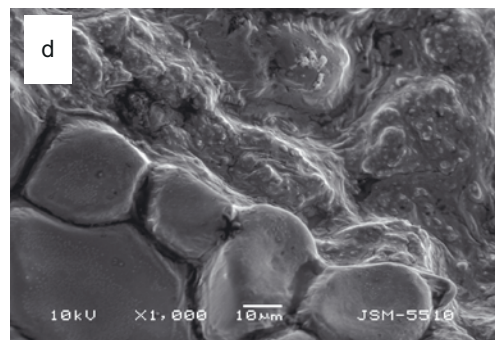
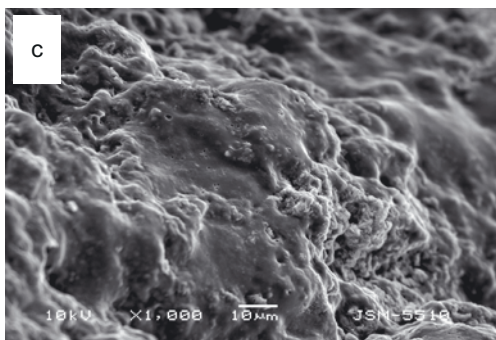
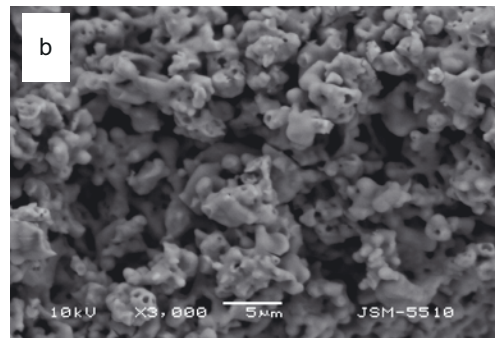
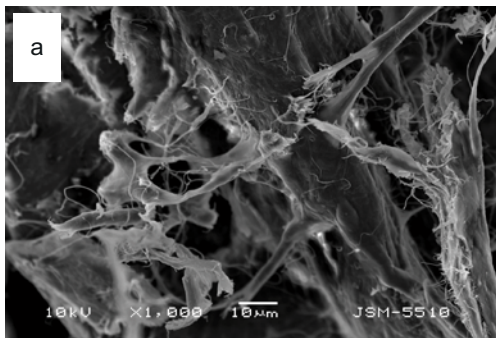


**Figure 7.** SEM images on collagen CPS/W hybrids: pure collagen (a), CPS/W sample, thermal treated at 1200°C/2 h (b), C-CPS/W-75:25 wt.% before SBF (c), C-CPS/W-75:25 wt.% before SBF (d), C-CPS/W-75:25 wt.% after SBF (e), C-CPS/W-25:75 wt.% after SBF (f)

From the presented XRD data it is clear that the X-ray diffraction patterns are quite different. In the case of C-CPS/W (25:75 wt.%) hybrid (Fig. 5) the obtained hydroxyapatite (PDF 00-8346) has a high crystallinity. On the other hand, the crystallinity of the  $\text{Ca}_{15}(\text{PO}_4)_2(\text{SiO}_4)_6$ , wollastonite and pseudowollastonite decreased after immersion of the prepared hybrid in 1.5 SBF for 3 days. In the case of C-CPS/W (75:25 wt.%) the crystallinity of obtained hydroxyapatite (Fig. 6) was lowest. In the same sample the wollastonites phase was not observed after immersion in 1.5 SBF, *i.e.* wollastonite fully dissolves in SBF solution for the immersion time. As can be seen, in two synthesized and immersed samples, XRD detects the presence of collagen amorphous halo.

SEM of pure collagen (Fig. 7a) can be characterized by fiber structure, which is visibly recognized. CPS/W (Fig. 7b) shows a visibly porous structure, which is a characteristic for silicon containing apatites [41]. When collagen was mixed CPS/W in 75:25 wt.%, SEM images (Fig. 7c) display that the collagen fully covered the CPS/W ceramic. When the quantity of collagen decreased to 25 wt.%, CPS/W ceramic was embedded into the collagen matrix (Fig. 7d).

The surface morphology of the obtained hybrids after soaking in 1.5 SBF (Figs. 7e,f) depicts that the surface was covered by a new hydroxyapatite layer.

## 4. Conclusions

The purposes of the present article were to prepare and to evaluate the *in vitro* bioactivity of hybrids between collagen and calcium phosphate silicate/wollastonite (CPS/W) glass-ceramics in Kokubo solution (1.5 SBF).

### References

- [1] A.C. Lowson, J. Chernuszka, Proc. Instr. Mech. Eng. 212, 413 (1998)
- [2] K. Burg, S. Porter, J. Kelman, Biomaterials 21, 2347 (2000)
- [3] R. Pillar *et al.*, Biomaterials 22, 963 (2001)
- [4] W. Suchanek, M. Yoshimura, J. Mater. Res. 13, 94 (1998)
- [5] I. Asashina *et al.*, J. Med. Dent. Sci. 44, 63 (1997)
- [6] A. Reddi, Tissue Eng. 6, 351 (2000)
- [7] M. Mami *et al.*, Appl. Surf. Sci. 254, 7386 (2008)
- [8] L. Meseguer-Olmo *et al.*, Acta Biomaterialia 4, 1104 (2008)
- [9] Zh. Zhou *et al.*, Journal of University of Science and Technology Beijing, Mineral, Metallurgy, Material 15, 290 (2008)
- [10] A. Balamurugan *et al.*, Mater. Lett. 60, 3752 (2006)
- [11] A.I. Martín, A.J. Salinas, M. Vallet-Regí, J. Eur. Ceram. Soc. 25, 3533 (2005)
- [12] J. Gil-Albarova *et al.*, Biomaterials 25, 4639 (2004)
- [13] D. Eglin *et al.*, J. Mater. Sci.: Mater. Med. 17, 161 (2006)
- [14] S. Padilla *et al.*, Acta Biomaterialia 2, 331 (2006)
- [15] A. Reddi, Nat. Biotechnol. 16, 247 (1998)
- [16] B. Chevalley, D. Herbage, Med. Biol. Eng. Comput. 38, 211 (2000)
- [17] F. Hsu, S. Chueh, Y. Wang, Biomaterials 20, 1931 (1999)
- [18] M. Kikuchi *et al.*, Biomaterials 12, 393 (1999)
- [19] M. Chang *et al.*, J. Mater. Sci. Lett. 20, 1109 (2001)
- [20] M.C. Chang *et al.*, J. Mater. Sci.: Mater. Med. 13, 993 (2002)

The CPS/W bioactive ceramics were synthesized *via* polystep sol-gel route with Ca/P+Si molar ratio 1.89. Hydrochloric acid diluted type I collagen was mixed with CPS/W powder in 25:75 and 75:25 weight ratio without binding agents. The obtained mixture was readjusted with 25%  $\text{NH}_4\text{OH}$  to pH=9. Then the mixture was dried at 37°C for 12 h. FTIR study detects, that the “red shift” of the strong amide I band at 1656  $\text{cm}^{-1}$  (for pure collagen) to 1647  $\text{cm}^{-1}$  (for C-CPS/W 25:75 wt.%) and to 1654  $\text{cm}^{-1}$  (for C-CPS/W 75:25 wt.%), can also be assigned to the presence of chemical bond in the prepared materials. FTIR observations after *in vitro* testing proved that the carbonate containing hydroxyapatite ( $\text{CO}_3\text{HA}$ ) can be formed on the surface of the synthesized hybrids. The negatively charged carboxylate groups of the collagen surface may be responsible for deposition of HA. This fact was confirmed by the “red shift” of carboxylate groups of the collagen molecules in the FTIR spectra.  $\text{CO}_3\text{HA}$  consisted of B-type  $\text{CO}_3^{2-}$  ions ( $\text{CO}_3^{2-} \rightarrow \text{PO}_4^{3-}$ ). SEM micrographs depicted that the surfaces are covered by a new hydroxyapatite layer.

## Acknowledgements

The financial support of the Bulgarian NSF under contract № VU-TN-102/2005 is gratefully acknowledged.

## In Memoriam

The publication of this work is dedicated to prof. Bisserka Samuneva, who passed away on November 19, 2008.

- [21] S.-H. Rhee, Y. Suetsugu, J. Tanaka, *Biomaterials* 22, 2843 (2001)
- [22] M. Kikuchi et al., *Composite Science and Technology* 64, 819 (2004)
- [23] S. Satome et al., *Materials Science and Engineering C* 24, 34 (2004)
- [24] S. Liao et al., *J. Biomed. Mater. Res. Part B: Appl. Biomater.* 74B, 817 (2005)
- [25] S. Yunoki et al., *J. Nanosci. Nanotechnol.* 7, 818 (2007)
- [26] M. Chang, J. Tanaka, *Biomaterials* 23, 4811 (2002)
- [27] M. Kikuchi et al., *Biomaterials* 25, 63 (2004)
- [28] G. Gafni, D. Sptier, M. Goldberg, *Journal of Crystal Growth* 205, 618 (1999)
- [29] E. Cowles, L. Brailey, G. Gronowicz, *J. Biomed. Mater. Res.* 52, 725 (2000)
- [30] A. Bellahcane et al., *Circ. Res.* 86, 885 (2000)
- [31] E. Sachlos et al., *Acta Biomaterialia* 4, 1322 (2008)
- [32] X. Li, J. Chang, *J. Mater. Sci.: Mater. Med.* 16, 361 (2005)
- [33] A. Monkawa et al., *Mater. Lett.* 60, 3647 (2006)
- [34] S.-H. Teng et al., *Mater. Lett.* 62, 3055 (2008)
- [35] C. Silva et al., *J. Mater. Sci.* 37, 2061 (2002)
- [36] L. Sukhodub et al., *Jornal of Molecular Structure* 704, 53 (2004)
- [37] H. Ishikawa et al., *Biomaterials* 22, 1689 (2001)
- [38] J. Grimes, T. Bocklage, J. Pitcher, *Orthopedics* 29, 145 (2006)
- [39] F. Schwarz et al., *Int. J. Oral. Maxillofac. Surg.* 36, 1198 (2007)
- [40] L. Pang et al., *Journal of US-China Medical Science* 4, 17 (2007)
- [41] M.H. Santos, H.S. Mansur, *Mater. Res.* 10, 431 (2007)
- [42] L. Radev et al., *Cent. Eur. J. Chem.* 7, 317 (2009)
- [43] G. Falini, M. Gazzano, A. Ripamonti, *J. Mater. Chem.* 10, 535 (2000)
- [44] W. Zhang et al., *J. Am. Ceram. Soc.* 86, 1052 (2003)
- [45] W.G. Mumme et al., *N. Jb. Miner. Abh.* 169, 35 (1995)
- [46] X.W. Li, H. Yasuda, Y. Umacoshi, *J. Mater. Sci.: Mater. Med.* 17, 573 (2006)
- [47] H.-S. Ryu et al., *J. Mater. Res.* 20, 1154 (2005)
- [48] F. Barba, P. Callejas, *J. Mater. Sci.* 41, 5227 (2006)
- [49] J. Vandiver et al., *J. Biomed. Mater. Res.* 78A, 352 (2006)
- [50] V. Jokanovic et al., *J. Mater. Sci.: Mater. Med.* 17, 539 (2006)
- [51] I. Hofmann et al., *J. Am. Ceram. Soc.* 90, 821 (2007)
- [52] N. Higon et al., *Chem. Mater.* 16, 1451 (2004)
- [53] I. Rehman, W. Bonfield, *J. Mater. Sci.: Mater. Med.* 8, 1 (1997)
- [54] I. Plyusnina, *Infrared spectra of silicates* (Mosk. Univ. Publ., Moscow, 1967) (In Russian)
- [55] I.R. Gibson, S.M. Best, W. Bonfield, *J. Biomed. Mater. Res.* 44, 422 (1999)
- [56] P. Richet, B. Mysen, J. Ingrin, *Phys. Chem. Minerals* 25, 401 (1998)
- [57] V. Swanmy, L. Dubrovinsky, F. Tutti, *J. Am. Ceram. Soc.* 80, 2237 (1997)
- [58] S. Langstaff, PhD Thesis, Queen's University, Canada 96 (1998)
- [59] F. Dong et al., *Journal of Wuhan University of Technology-Mater. Sci. Ed.* 19, 94 (2004)
- [60] E. Landi et al., *J. Eur. Ceram. Soc.* 23, 2931 (2003)
- [61] J.C. Marry et al., *J. Mater. Sci.: Mater. Med.* 9, 79 (1998)
- [62] A.J. Salinas, M. Valett-Regi, I. Izquierdo-Barba, *J. Sol-Gel Sci. Techn.* 21, 13 (2001)
- [63] M. Cerruti, D. Greenspan, K. Powers, *Biomaterials* 26, 4903 (2005)
- [64] S. Federman et al., *Mater. Res.* 10, 177 (2007)
- [65] M. Cerruti et al., *J. Mater. Chem.* 13, 1279 (2003)
- [66] M. Vallet-Regi et al., *Chem. Mater.* 17, 1874 (2005)
- [67] A. Martinez, I. Barba, M. Vallet-Regi, *Chem. Mater.* 12, 3080 (2000)
- [68] K. Payne, A. Vies, *Biopolymers* 27, 1749 (1988)
- [69] M. Chang, C. Ko, W. Douglas, *Biomaterials* 24, 2853 (2003)
- [70] X. Yang et al., *Materials Science and Engineering C* 29, 25 (2009)
- [71] J.P. Lafon, E. Champion, D. Bernache-Assolant, *J. Eur. Ceram. Soc.* 28, 139 (2008)
- [72] A. Ramila, F. Balas, M. Vallet-Regi, *Chem. Mater.* 14, 542 (2002)
- [73] M. Vallet-Regi, A. Ramila, *Chem. Mater.* 12, 961 (2000)
- [74] N. Colleman et al., *Ceramics-Silikaty* 51, 1 (2007)
- [75] A. Balamurugan et al., *J. Biomed. Mater. Res. Part B: Appl. Biomater.* 83B, 546 (2007)
- [76] K. Liu et al., *Biochim. Biophys. Acta* 4, 73 (1996)
- [77] M.H. Santos, L. Hermeine, H. Mansur, *Mater. Sci. Eng. C* 28, 568 (2008)
- [78] Li-J. Zhang et al., *Mater. Lett.* 58, 719 (2004)
- [79] M. Kikuchi et al., *Biomaterials* 22, 1705 (2001)
- [80] J. Baralen, S. Best, W. Bonfield, *J. Biomed. Mater. Res.* 41, 79 (1998)